Sol-gel synthesis and nonlinear optical transmission in $Zn_{(1-x)}Mg_{(x)}O$ ($x \leqslant 0.2$) thin films

C. S. Suchand Sandeep and Reji Philip[a)]
Raman Research Institute, C. V. Raman Avenue, Sadashiva Nagar, Bangalore 560 080, India

R. Satheeshkumar and V. Kumar
Centre for Materials for Electronics Technology, Mulangunnathukavu, Thrissur 680 771, India

(Received 15 December 2005; accepted 21 June 2006; published online 7 August 2006)

Nanocrystalline $Zn_{1-x}Mg_xO$ thin films with an average particle diameter of 60 nm have been deposited on glass substrates using a sol-gel spin-coating technique. Within the range of compositions, $0 \leqslant x \leqslant 0.20$, the optical band gap could be tuned between 3.40 and 3.83 eV. The nonlinear optical transmission in the visible spectral region is investigated using ultrafast (100 fs) and short (7 ns) laser pulses at off-resonant wavelengths. The observed nonlinearity is strong and is comparable to that recently obtained in ZnO nanocomposite layers ion-implanted with Cu^+ ions.
 [DOI: 10.1063/1.2335375]

Even though most electrical conductors are opaque, and most optically transparent solids are electrical insulators, post-transition-metal oxides and their alloys are an exception. Despite their large band gaps, which render transparency under normal conditions, they also possess a high electrical conductivity and sustain a high concentration of electrons with high carrier mobility. Some examples are oxides of *p* block metals such as ZnO, In_2O_3, SnO_2, and their alloys. The electronic structure of these crystals is characterized by a wide band gap of over 3.0 eV and highly concentrated donor levels of oxygen defects just below the conduction band. The wide gap causes transparency in the visible region, and electrons at the shallow donor levels provide electrical conductivity. These materials are known as transparent conducting oxides (TCOs). TCOs are used in optoelectronic devices such as flat-panel displays, windshield defrosters, and solar cells. In particular, ZnO finds potential applications in transparent electronics, spintronics, data storage, UV light emitters, chemical and gas sensors, surface acoustic wave devices, and transparent contacts.[1–7]

A number of nonlinear optical measurements have been done in TCO films to investigate their second and third order nonlinearities.[8–11] In this letter we report the preparation of nanocrystalline $Zn_{1-x}Mg_xO$, $x \leqslant 0.20$, thin films on glass substrates using a sol-gel spin-coating technique. Within the range of compositions, $0 \leqslant x \leqslant 0.20$, the optical band gap is tunable between 3.40 and 3.83 eV. We investigated the nonlinear optical transmission of these samples in the visible spectral region using ultrafast (100 fs) and short (7 ns) laser pulses, at the off-resonant wavelengths of 800 and 532 nm, respectively. The nonlinearity was found to be of the induced absorption type in both cases.

Commercially available acetates of zinc and magnesium were used as the starting materials. Sol stabilizer, acetyl acetone equimolar to the $[Zn^{2+}+Mg^{2+}]$, was used to prepare stable solutions in isopropyl alcohol solvent. 20 μl of the solution was used for spin-coating $Zn_{1-x}Mg_xO$ thin films on commercially available glass substrates at 2000 rpm. The coated substrate was then dried at 110 °C for half an hour and then placed in a furnace and annealed in air atmosphere at 600 °C for half an hour. This cycle was repeated several times to obtain films of desired thickness. Prior to spin coating, the substrates were cleaned using a sonicator in water and alcohol, and dried. The prepared coatings are transparent on visual inspection.

The absorption spectra in the visible region (Fig. 1) were recorded on a UV/VIS/NIR spectrophotometer (JASCO V-570). It is seen that the absorption maxima get blueshifted as a function of the Mg content. The absorption maxima and the band gap (E_g) are given in Table I. E_g increases up to 3.83 eV within the range of composition studied, $0 \leqslant x \leqslant 0.20$.

An order of magnitude estimate of the grain size is possible from the absorption spectra. When compared to the absorption maximum of bulk ZnO (3.37 eV; 369 nm), the same is blueshifted to 3.40 eV (366 nm) in the nanostructured ZnO thin film. By the quantum size effect in nanosized semiconductors,[12] the band gap increases when the size of the particle is decreased, resulting in a blueshift of absorption bands. From the effective mass approximation (EMA) relation and the absorption spectrum of the sample, the particle size $D=2R$ of ZnO can be estimated to be 14 nm. The model developed by Viswanatha *et al.*[13] gives a close value

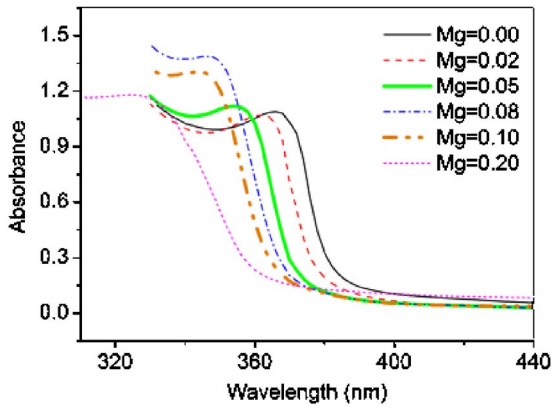

FIG. 1. (Color online) Absorption spectra of $(Zn_{1-x}Mg_x)O$ thin films.

[a)]Author to whom correspondence should be addressed; electronic mail: reji@rri.res.in

TABLE I. Lattice parameters, band gap energy, and nonlinear optical coefficients obtained for the $(Zn_{1-x}Mg_x)O$ thin films.

Film	c (Å)	A (Å)	Volume (Å^3)	λ_{max} (nm)	E_g (eV)	β (10^{-6} m/W)	γ (10^{-27} m^3/W^2)
$x=0$	5.21	3.26	143.85	366	3.40	4.3	2.0
$x=0.02$	5.21	3.26	143.85	362	3.43	4.6	2.4
$x=0.05$	5.22	3.26	144.13	354	3.47	5.0	···
$x=0.08$	5.22	3.26	144.13	346	3.59	5.8	3.4
$x=0.10$	5.18	3.24	141.27	344	3.61	6.5	5.1
$x=0.20$	5.25	3.25	141.27	324	3.83	···	6.1

of $D=10$ nm. To compare these estimates with the actual values, we recorded the microstructure of the thin films using a scanning electron microscope (SEM, S-4300 Hitachi). The cross-sectional SEM image for an undoped ZnO thin film on a glass substrate is given in Fig. 2. It indicates a well densified uniform microstructure with an average grain diameter of 60 nm. The thickness of a single layer corresponds almost to the average grain diameter.

The crystalline phases were detected with an x-ray diffractometer (XRD, Bruker model D-5000) with Cu $K\alpha$ radiation. Figure 3 shows the XRD patterns of $Zn_{1-x}Mg_xO$ thin films annealed at 600 °C in air. All patterns indicate the formation of the single wurzite-type ZnO phase. No evidence of MgO phase was seen, confirming the monophasic nature of these compositions (Ohtomo *et al.*[14] have reported a solid solubility of ~35% of MgO in ZnO in pulsed laser deposited thin films). Thin films with x up to 0.20 exhibited a preferred c-axis orientation, whereas for compositions with $x \geqslant 0.20$, the patterns were similar to that of bulk ZnO. The lattice constants derived from the XRD are given in Table I as a function of the Mg content. Since the ionic radii of Mg^{2+} and Zn^{2+} are nearly equal, the hexagonal cell volume is hardly changed.

The mean crystallite size of the films were evaluated using the EMA relationship and the tight binding model of Valence Band and Conduction Band (Refs. 13 and 15–17) from the ΔE_g (the shift in E_g from the bulk value for coarse ZnO) values. Film thickness and refractive index were evaluated from the interference bands in the transmittance spectra of the films on glass substrates using the envelope method.[18]

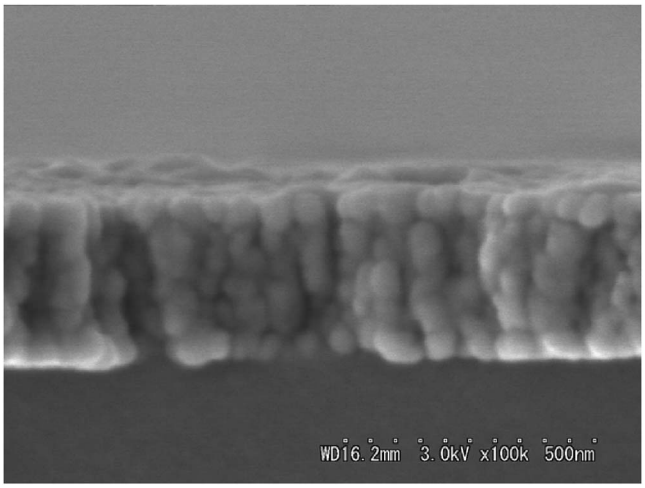

FIG. 2. Cross-sectional SEM image of an undoped ZnO thin film on glass substrate.

The nonlinear optical transmission in the films was investigated using an open aperture z-scan setup,[19] which is automated, and uses two pyroelectric energy probes. In the z scan, the laser beam is focused using a lens and the sample is translated along the laser beam axis (called the z direction) so that it passes through the focal point ($z=0$) during the motion. For each z value the sample will see a different laser energy density, and the sample transmission for different z values is measured using a laser energy meter. We used the wavelengths of 532 and 800 nm for excitation. Laser pulses of 100 fs duration at 800 nm were obtained from a Ti:sapphire chirped pulse amplification laser system (TSA-10, Spectra Physics). 532 nm, 7 ns pulses were obtained from a frequency-doubled neodymium-doped yttrium aluminum garnet laser. By using these different pulse widths, a large range in the applied optical intensity could be achieved. The laser pulse repetition rate is ~1 Hz.

Some of the nonlinear transmittance curves extracted from the z-scan data are shown in Fig. 4. It is found that the net transmission T of the films can be described by a two-photon absorption process given by[20]

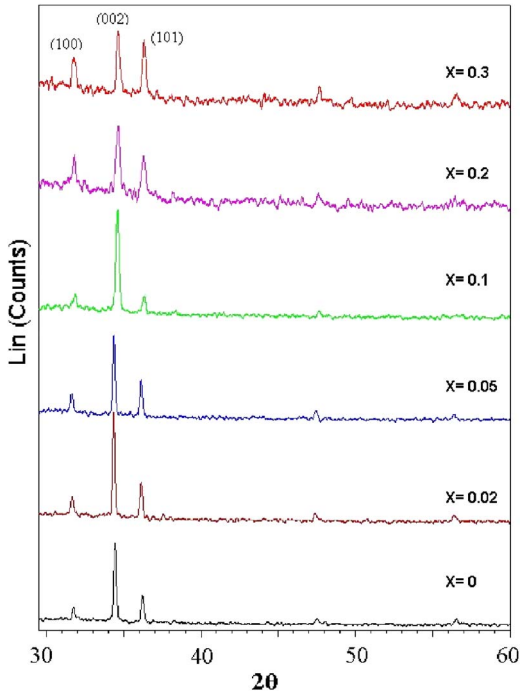

FIG. 3. (Color online) XRD patterns of $(Zn_{1-x}Mg_x)O$ thin films annealed at 600 °C in air.

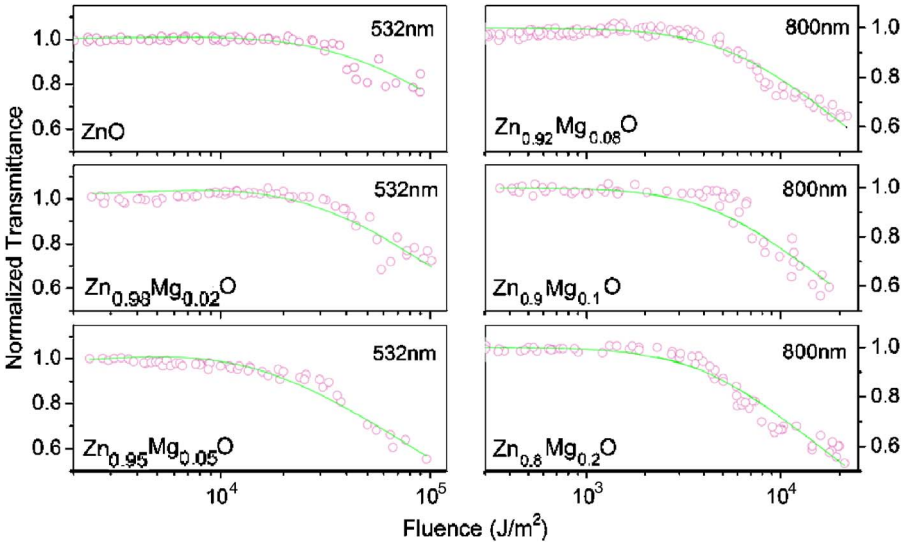

FIG. 4. (Color online) Normalized transmittance of the films as a function of input fluence. The circles are experimental data, while solid curves are theoretical fits. For 532 nm excitation, data are fitted for a two-photon process using Eq. (1). For 800 nm excitation, data are fitted for a three-photon process using Eq. (2).

$$T = ((1-R)^2 \times \exp(-\alpha L)/\sqrt{\pi} q_0) \int_{-\infty}^{+\infty} \ln[\sqrt{1+q_0 \exp(-t^2)}]dt \quad (1)$$

at 532 nm, and by a three-photon process given by

$$T = ((1-R)^2 \times \exp(-\alpha L)/\sqrt{\pi} p_0) \int_{-\infty}^{+\infty} \ln[\sqrt{1+p_0^2 \exp(-2t^2)}] + p_0 \times \exp(-t^2)dt \quad (2)$$

at 800 nm. L and R are the sample length and surface reflectivity, respectively, and α is the linear absorption coefficient. q_0 in Eq. (1) is given by $\beta(1-R)I_0 L_{\text{eff}}$, where β is the two-photon absorption coefficient and I_0 is the on-axis peak intensity. L_{eff} is given by $[1-\exp(-\alpha L)]/\alpha$. p_0 in Eq. (2) is given by $[2\gamma(1-R)^2 I_0^2 L'_{\text{eff}}]^{1/2}$, where γ is the three-photon absorption coefficient and L'_{eff} is given by $[1-\exp(-2\alpha L)]/2\alpha$. The numerically calculated values of β and γ are shown in Table I. From a number of z scans obtained for each sample, it is estimated that the β values lie within an error bar of ±20%, while that of γ values is ±30%. Even then, the nonlinearity obviously shows an increasing trend with the Mg content in the films. The β values obtained are quite high, and are of the same order of magnitude as those obtained by Ryasnyansky *et al.*,[21] for similarly irradiated ZnO nanocomposite layers (prepared by ion implantation) doped with Cu nanoparticles. For $x=0.2$, β could not be calculated, and for $x=0.05$, γ could not be calculated, due to a larger than acceptable scattering in the z-scan data.

The observed three-photon nonlinearity at 800 nm can be caused by a pure three-photon process, as well as a two-photon-induced free-carrier absorption[20] process. From the absorption spectra it is clear that a two-photon absorption at 800 nm (equivalent to a single 400 nm photon) will raise an electron to the long wavelength absorption tail of the band gap (lowermost levels of the conduction band). Considering the dense donor levels of oxygen defects just below the conduction band, free carrier absorption from these levels can become quite significant.

In conclusion, we have reported the sol-gel deposition of nanostructured $Zn_{1-x}Mg_xO$ thin films on glass substrates by the spin-coating method. It is found that the films are c-axis oriented up to $x=0.20$. A strong optical nonlinearity of the induced absorption type is found in the films in the off-resonant excitation region for ultrafast as well as short laser pulse excitation. Since the band edge of the films is close to 400 nm, it is likely that the observed nonlinearity at 800 nm has a contribution from two-photon-induced free-carrier absorption. The measured third order nonlinear absorption coefficients at 532 nm are of the same order of magnitude as those found for nanocomposite ZnO layers implanted with Cu^+ ions, excited under similar conditions.

[1] D. C. Look, Mater. Sci. Eng., B **80**, 383 (2001).
[2] Ya. I. Alivov, E. V. Kalinina, A. E. Cherenkov, D. C. Look, B. M. Ataev, A. K. Omaev, M. V. Chukichev, and D. M. Bagnall, Appl. Phys. Lett. **83**, 4719 (2003).
[3] T. Yatsui, J. Lim, M. Ohtsu, S. J. An, and G.-C. Yi, Appl. Phys. Lett. **85**, 727 (2004).
[4] A. Ohtomo, M. Kawasaki, I. Ohkubo, H. Koinuma, T. Yasuda, and Y. Segawa, Appl. Phys. Lett. **75**, 980 (1999).
[5] A. K. Sharma, J. Narayan, J. F. Muth, C. W. Teng, C. Jin, A. Kvit, R. M. Kolbas, and O. W. Holland, Appl. Phys. Lett. **75**, 3327 (1999).
[6] C. W. Teng, J. F. Muth, U. Ozgur, M. J. Bergmann, H. O. Everitt, A. K. Sharma, C. Jin, and J. Narayan, Appl. Phys. Lett. **76**, 979 (2000).
[7] S. Z. Weisz, O. Resto, G. Yaron, A. Many, and H. Y. Goldstein, J. Vac. Sci. Technol. A **5**, 302 (1987).
[8] W. Wang, J. Xu, X. Liu, Y. Jiang, G. Wang, and X. Lu, Acta Opt. Sin. **20**, 1421 (2000).
[9] M. C. Larciprete, D. Passeri, F. Michelotti, S. Paoloni, C. Sibilia, M. Bertolotti, A. Belardini, F. Sarto, F. Somma, and S. Lo Mastro, J. Appl. Phys. **97**, 023501 (2005).
[10] A. Narazaki, T. Hirano, J. Sasai, K. Tanaka, and K. Hirao, Mater. Res. Soc. Symp. Proc. **607**, 421 (2000).
[11] J. Han, H. Zhou, and Q. Wang, Mater. Lett. **60**, 252 (2005).
[12] A. P. Alivisatos, J. Phys. Chem. **100**, 13226 (1996).
[13] R. Viswanatha, S. Sapra, B. Satpati, P. V. Satyam, B. N. Dev, and D. D. Sharma, J. Mater. Chem. **14**, 661 (2004).
[14] A. Ohtomo, M. Kawasaki, T. Koida, K. Masubuchi, H. Koinuma, Y. Sakurai, Y. Yoshida, T. Yasuda, and Y. Segawa, Appl. Phys. Lett. **72**, 2466 (1998).
[15] L. E. Brus, J. Chem. Phys. **79**, 5566 (1983).
[16] N. Chestnoy, R. Hall, and L. E. Brus, J. Chem. Phys. **85**, 2237 (1986).
[17] P. E. Lippens and M. Lannoo, Phys. Rev. B **39**, 10935 (1989).
[18] J. C. Manifacier, J. Gasiot, and J. P. Fillard, J. Phys. E **9**, 1002 (1976).
[19] M. Sheik Bahae, A. A. Said, T. H. Wei, D. J. Hagan, and E. W. Van Stryland, IEEE J. Quantum Electron. **26**, 760 (1990).
[20] R. L. Sutherland, *Handbook of Nonlinear Optics*, 2nd ed. (Dekker, New York, 2003), Chap. 9, pp. 583 and 591.
[21] A. Ryasnyansky, B. Palpant, S. Debrus, R. Ganeev, A. Stepanov, N. Can, C. Buchal, and S. Uysal, Appl. Opt. **44**, 2839 (2005).